

Published in final edited form as:

*J Cell Sci.* 2008 March 15; 121(0 6): 753–761. doi:10.1242/jcs.017681.

## Signal-dependent export of GABA transporter 1 from the ER-Golgi intermediate compartment is specified by a C-terminal motif

Hesso Farhan<sup>1</sup>, Veronika Reiterer<sup>1</sup>, Alexander Kriz<sup>2</sup>, Hans-Peter Hauri<sup>2</sup>, Margit Pavelka<sup>3</sup>, Harald H. Sitte<sup>1</sup>, and Michael Freissmuth<sup>1,\*</sup>

<sup>1</sup>Institute of Pharmacology, Center of Biomolecular Medicine and Pharmacology, Medical University of Vienna, Waehring Str. 13a, 1090 Vienna, Austria <sup>2</sup>Department of Pharmacology and Neurobiology, Biozentrum, University of Basel, Klingelbergstrasse 70, CH-4056 Basel, Switzerland <sup>3</sup>Department of Cell Biology and Ultrastructure Research, Center for Anatomy and Cell Biology, Medical University of Vienna, Schwarzschanerstr. 17, A-1090 Vienna, Austria

### Summary

The C-terminus of GABA transporter 1 (GAT1, SLC6A1) is required for trafficking of the protein through the secretory pathway to reach its final destination, i.e. the rim of the synaptic specialization. We identified a motif of three hydrophobic residues (<sup>569</sup>VMI<sup>571</sup>) that was required for export of GAT1 from the ER-Golgi intermediate compartment (ERGIC). This conclusion was based on the following observations: (i) GAT1-SSS, the mutant in which <sup>569</sup>VMI<sup>571</sup> was replaced by serine residues, was exported from the ER in a COPII-dependent manner but accumulated in punctate structures and failed to reach the Golgi; (ii) under appropriate conditions (imposing a block at 15°C, disruption of COPI), these structures also contained ERGIC53; (iii) the punctae were part of a dynamic compartment, because it was accessible to a second anterograde cargo [the temperature-sensitive variant of vesicular stomatitis virus G protein (VSV-G)] and because GAT1-SSS could be retrieved from the punctate structures by addition of a KKxx-based retrieval motif, which supported retrograde transport to the ER. To the best of our knowledge, the VMI-motif of GAT1 provides the first example of a cargo-based motif that specifies export from the ERGIC.

### Keywords

GABA transporter-1; ER-to-Golgi trafficking; ERGIC

### Introduction

Export of proteins from the endoplasmic reticulum (ER) is mediated by COPII-coated vesicles, which bud from so-called ER exit sites (ERES). In mammalian cells, unlike in yeast, COPII vesicles are not directly delivered to the Golgi. Instead, they fuse homotypically to generate the ER-Golgi intermediate compartment (ERGIC) (Xu and Hay,

\* Author for correspondence (michael.freissmuth@meduniwien.ac.at).

2004; Yu et al., 2006). The ERGIC is a compartment in which sorting decisions are made (Appenzeller-Herzog and Hauri, 2006). It is a matter of debate how cargo is transported from the ERGIC to the Golgi, and there exist two rivaling theories on the nature of the ERGIC (Hauri et al., 2000). The maturation hypothesis assumes that the ERGIC is not a true compartment but rather an accumulation of membranes on their way to the Golgi. These membranes are destined to fuse and generate the cis-Golgi network. In other words, transport between the ERGIC and the Golgi is thought to be mediated by en bloc movement of membrane containers (Horstmann et al., 2002). By contrast, the stationary-compartment hypothesis posits that the ERGIC is a stable compartment that has a highly dynamic turnover of components. This hypothesis is supported by the recent observation that anterograde and retrograde cargo segregate at the level of the ERGIC (Ben-Tekaya et al., 2005). The stationary-compartment hypothesis makes two predictions: (i) a specialized machinery is required to support the flow of membrane and thus the transport of cargo from the ERGIC to the Golgi; for instance, there must be coat proteins that allow for cargo selection and for vesicle budding. The nature of this machinery is unknown. However, there is evidence that COPI plays a major role in this process: cargo transport is blocked at the level of the ERGIC if COPI is inactivated (Pepperkok et al., 1993; Gomez et al., 2000). (ii) Export from the ERGIC should be specified by the cargo molecule, i.e. the cargo protein must contain motifs that allow for recruitment of the export machinery in a manner analogous to that for ER export.

In the current work, we investigated ER-to-Golgi trafficking of GABA transporter 1 (GAT1, SLC6A1), a member of the SLC6 gene family of Na<sup>+</sup>/Cl<sup>-</sup>-dependent neurotransmitter transporters. Our previous work showed that the C-terminus of GAT1 contained several motifs that controlled its subcellular localization (Farhan et al., 2004; Farhan et al., 2007). Efficient export from the ER is specified by the <sup>566</sup>RL<sup>567</sup> motif, which mediates the interaction with Sec24D. Here, we focus on an adjacent trihydrophobic motif (<sup>569</sup>VMI<sup>571</sup>), which is also essential for cell-surface localization: disruption of the motif by serine substitution caused retention of the resulting mutant GAT1-SSS in the ERGIC. Thus, a specific motif is required for exit of GAT1 from the ERGIC.

## Results

### GAT1-SSS is localized in a post-ER compartment

We previously showed that mutation of the <sup>569</sup>VMI<sup>571</sup> to serines led to intracellular retention of GAT1 but did not affect its interaction with Sec24D (Farhan et al., 2004; Farhan et al., 2007). GAT1-SSS was visualized in peripheral punctate structures and in a perinuclear dense region (Fig. 1B). This pattern was seen in the vast majority of cells (~82%, 75/92 cells that were scored). Because GAT1-SSS interacts with the COPII coat (Farhan et al., 2007), we surmised that these punctae were not contiguous with the ER. This assumption was tested using two approaches: (i) by colocalization with the ER-resident protein reticulon (Fig. 1C) or with an ER-specific dye (not shown); and (ii) by employing fluorescence recovery after photobleaching (FRAP). GAT1-SSS-containing punctae (Fig. 1C, middle panel) did not colocalize with reticulon 2 (Fig. 1C, left-hand panel), resulting in segregation of false-colour pixels upon overlay of the images (Fig. 1C, right-hand panel).

GAT1-SSS also did not colocalize with the ER-specific dye (data not shown). Similarly, if YFP-tagged GAT1-SSS proteins were photobleached, fluorescence did not recover over the time course investigated (Fig. 1D, upper panel). As a control, we employed GAT1-RL/AS; this mutant is predominantly trapped in the ER (because it does not bind Sec24D) (see Farhan et al., 2007); as expected for an ER-resident protein, fluorescence emission by GAT1-RL/AS rapidly recovered by lateral diffusion (Fig. 1D, lower panel). Based on these observations, we surmised that GAT1-SSS reached a post-ER compartment. Thus, the mutated protein should be capable of leaving the ER, if it accumulates in a post-ER compartment. To test this hypothesis, we performed an *in vitro* vesicle-budding assay. HEK293 cells were co-transfected with plasmids encoding YFP-GAT1-SSS or YFP-GAT1-37 together with Sar1-T39N. Because Sar1-T39N prevents COPII coat recruitment and ER exit-site formation in a dominant-negative manner, YFP-GAT1-SSS was retained in the ER (see below). The truncated mutant GAT1-37 (lacking the last 37 amino acids) was used as a control; this mutant lacks the Sec24D-binding motif and is trapped in the ER (Farhan et al., 2004). After 24 hours, cells were permeabilized and cytosol containing wild-type Sar1 was added to reconstitute vesicle budding: GAT1-SSS was efficiently incorporated into budding vesicles (Fig. 1E, cf. third and fourth lanes), whereas GAT1-37 was not (Fig. 1E, cf. seventh and eighth lane). As an additional control, the reaction was done on ice: under this condition, neither GAT1-SSS nor GAT1-37 proteins were incorporated into vesicles to any appreciable extent (Fig. 1E, lanes 1 and 2, and 5 and 6, respectively). Finally, we also verified the validity of the assay by using endogenous proteins: ERGIC53 (LMAN1) was released into vesicles at 37°C (Fig. 1F). By contrast, the ER-resident protein CLIMP63 (Schweizer et al., 1993) remained associated with the ER (Fig. 1G).

### **GAT1-SSS does not have a toxic effect on cells**

In contrast to GAT1-RL/AS, which eventually escapes from the ER in a non-concentrative manner and reaches the plasma membrane (Farhan et al., 2007), GAT1-SSS accumulated in these punctate structures and did not reach the plasma membrane even in stably transfected cells. Proteins that are retained in the early secretory pathway might exert a toxic effect because they are not readily cleared (e.g. by retrotranslocation through the Sec61 channel or other mechanisms of ER-associated degradation). Trembler J, a mutated version of the peripheral myelin protein-22 (PMP22), for instance, accumulates in the ERGIC and leads to morphological changes in the ER, i.e. its condensation (Tobler et al., 1999), that are indicative of a toxic effect. Accordingly, the membrane compartments and organelles of the early secretory pathway were investigated by electron microscopy in HEK293 cells stably expressing GAT1-SSS or wild-type GAT1. We focused specifically on the ER, ERGIC and the stacks of the Golgi apparatus. Our studies showed that these compartments were intact in both HEK293 cells expressing wild-type GAT1 (Fig. 2A) and GAT1-SSS (Fig. 2B). The ultrastructures of the early secretory compartments in cells expressing GAT1-SSS were indistinguishable from those visualized in the wild-type GAT1 cells. Hence, we did not find any indication for toxic effects of GAT1-SSS.

### **Formation of the GAT1-SSS punctae is dependent on COPII**

As shown above, GAT1-SSS leaves the ER via vesicular carriers. Because GAT1-SSS binds COPII, we surmised that the formation of GAT1-SSS punctae is dependent on COPII. This

was tested by three different approaches: (i) HEK293 cells were transiently transfected with a plasmid encoding YFP-tagged GAT1-SSS and treated overnight with the kinase inhibitor H89, which blocks COPII-mediated ER export (Aridor and Balch, 2000). Treatment with H89 prevented formation of GAT1-SSS punctae and the mutant was localized in the ER (Fig. 3C). (ii) A similar result was obtained when GAT1-SSS was co-expressed with SAR1A-T39N (Fig. 3B). (iii) Dominant-negative SAR1A1 results in an overall inhibition of COPII function and, accordingly, traps all membrane proteins that are destined for concentrative export in the ER. As a more specific inhibitor, we co-expressed GAT1-SSS with Sec24D-VN. This mutant of Sec24D does not bind GAT1 and thus blocks its ER export; Sec24D-VN, however, does not impede ER export of other (model) cargoes such as VSVG-ts045 (Farhan et al., 2007). Sec24D-VN also prevented formation of GAT1-SSS punctae (Fig. 3C). Finally, we reasoned that mutation of the Sec24D-interaction motif (<sup>566</sup>RL<sup>567</sup>) in GAT1-SSS should act as a second site suppressor. This was the case: GAT1-RL/AS-SSS was visualized predominantly in the ER rather than in punctate structures. Low amounts were also visible at the plasma membrane (Fig. 3D). This pattern of distribution is the same as for GAT1-RL/AS, which reaches the plasma membrane by bulk flow rather than concentrative export (Farhan et al., 2007). Thus, we conclude that formation of GAT1-SSS-containing punctae is dependent on COPII. We further ruled out that intracellular retention of GAT1-SSS was due to misfolding and association with (unidentified) chaperons. If GAT1-SSS were misfolded and aggregated into large complexes by chaperons, its mobility in the ER ought to be slower compared to that of the wild-type protein. This was tested in FRAP experiments with HEK293 cells co-expressing either wild-type GAT1 or GAT1-SSS together with SAR1A-T39N. We did not detect any difference in the half-lives of fluorescence recovery between the two proteins (Fig. 3D), indicating that GAT1-SSS was not trapped by association with chaperons.

### **GAT1-SSS does not colocalize with known markers of ERES, the ERGIC and the Golgi**

Staining of the peripheral punctae is reminiscent of either ERES or of the ERGIC. Alternatively, these punctae could represent endosomes/lysosomes. By contrast, the perinuclear dense region was compatible with the Golgi. We characterized the compartment in which GAT1-SSS was retained by transfecting HeLa cells with plasmids encoding YFP-tagged GAT1-SSS followed by immunostaining: after 24 hours, cells were fixed and stained against Sec31 (to label ERES, Fig. 4A), GM130 (a marker for the cis-Golgi, Fig. 4B) and LAMP1 (a marker for late endosomes and lysosomes, Fig. 4C). GAT1-SSS did not colocalize with either of these markers (Fig. 4A-C). We also excluded that the larger and brighter GAT1-SSS structures colocalized with LAMP-1: we acquired stacks every 160 nm that revealed that there was no colocalization between those proteins (see the lower part of Fig. 4C). We nevertheless noted that the peripheral GAT1-SSS punctae exhibited a close association with ERES (arrowhead in the rightmost image in Fig. 4A). The same has been observed with peripheral ERGIC structures. Therefore, we tested whether GAT1-SSS was localized in the ERGIC by colocalizing it with ERGIC53, the eponymous marker for this compartment. HeLa cells expressing YFP-tagged GAT1-SSS were fixed and ERGIC53 was detected by immunofluorescence. GAT1-SSS did not colocalize with ERGIC53 (Fig. 4D).

## GAT1-SSS is localized in the ERGIC

The findings summarized in Fig. 4 can be rationalized by the following scenario: GAT1-SSS leaves the ER via COPII-coated vesicles, which fuse homotypically or with pre-existing 'membrane containers' of the ERGIC. As an anterograde secretory cargo, GAT1 does not carry retrieval motifs and thus remains in these containers; because the mutation in GAT1-SSS prevents exit from these membrane containers, they represent a cul-de-sac for the mutated protein. By contrast, ERGIC53 recycles very actively between the ER and the ERGIC. This is one possible explanation for a lack of colocalization of GAT1-SSS with ERGIC53. If this interpretation were true, inhibition of ERGIC53 recycling should result in colocalization of the two proteins. One way to block ERGIC53 recycling is incubation of the cells at 15°C. Therefore, we incubated HEK293 cells expressing cyan fluorescent protein (CFP)-GAT1-SSS together with green fluorescent protein (GFP)-ERGIC53 at 15°C for 2 hours. This treatment caused the two proteins to colocalize (Fig. 5A). A second approach was also used to corroborate these findings: IdIF cells carry a mutation in the *e-COP* gene, which renders the protein temperature-sensitive. Incubation of cells at 40°C for 2-3 hours leads to inhibition of COPI activity by 90%. When IdIF cells expressing CFP-GAT1-SSS and GFP-ERGIC53 were kept at the restrictive temperature, the two proteins colocalized (Fig. 5B). GM130, a Golgi matrix protein, localizes to the ERGIC after treatment with brefeldin A (BFA) (Nakamura et al., 1995). Therefore, we treated HeLa cells expressing yellow fluorescent protein (YFP)-tagged GAT1-SSS with BFA for 10 minutes. Cells were fixed and GM130 was detected by immunofluorescence. As shown in Fig. 4B, GAT1-SSS did not colocalize with GM130 in untreated cells. However, there was a prominent colocalization between GAT1-SSS and GM130 when the latter was driven to localize to the ERGIC after treatment with BFA (Fig. 5C).

Sannerud et al. (Sannerud et al., 2006) showed that PC12 cells expand their ERGIC while developing neurite extensions upon differentiation: whereas ERGIC53-positive IC elements remain in the cell body, RAB1-containing tubules extend to the growth cones of the neurite extensions. We previously reported that GAT1 is enriched in the growth cone and in the neurite extension of PC12 cells (Farhan et al., 2004). We therefore tested whether (i) the formation of GAT1-SSS punctae was dependent on RAB1 and (ii) whether GAT1-SSS colocalized with RAB1. Accordingly, we transfected HEK293 cells with plasmids encoding YFP-tagged GAT1-SSS together with CFP-tagged RAB1-N121I (dominant-negative version of RAB1). After 24 hours, cells were fixed and the number of cells exhibiting a punctate staining of GAT1-SSS was evaluated. Co-expression of RAB1-N121I drastically reduced the number of cells with GAT1-SSS punctae from 81.5% (75/92 cells that were counted) down to 29% (27/93 cells that were counted). RAB1 can only be visualized in the IC when it is exogenously expressed, as has been reported by others (Alvarez et al., 2003; Monetta et al., 2007). We reasoned that, because RAB1 plays a role in ER-to-Golgi trafficking of GAT1, the IC-localized RAB1 ought to colocalize with GAT1-SSS. Therefore, we co-expressed YFP-tagged GAT1 and CFP-tagged RAB1A. CFPRAB1A appeared very sparsely in peripheral punctate structures and the staining intensity of these structures was low, making a colocalization difficult. However, among the RAB1-positive peripheral structures there was a good degree of colocalization with GAT1-SSS (40±5.9%; Fig. 5D). Taken

together, the data from Fig. 5A-D strongly argue in favour of GAT1-SSS localization in pre-Golgi intermediates that do not contain ERGIC53.

Trafficking of the temperature-sensitive variant VSVG-ts045 is blocked at the level of the ERGIC if COPI is inactivated (Pepperkok et al., 1993; Gomez et al., 2000). To test whether the same applies for GAT1, we transfected IdIF cells with plasmids encoding YFP-tagged GAT1 together with a plasmid encoding myc-tagged human ERGIC53. Cells were incubated overnight at 34°C before switching to the restrictive temperature (40°C) for 4 hours. Cells were then fixed and ERGIC53 was detected by immunofluorescence. As seen in Fig. 5E, GAT1 colocalized with ERGIC53 if COPI was inactivated. The results obtained in IdIF cells clearly indicate that COPI is important for trafficking of GAT1 from the ERGIC. This tempted us to speculate that a deficiency in COPI recruitment could underlie the trafficking defect of GAT1-SSS. This conjecture was verified by incubating GST-fusion proteins comprising the GAT1 C-terminus (wild type and the mutated version) with cytosol from HEK293 cells. The amount of COPI bound to the C-terminus was visualized by immunoblotting for  $\beta$ -COP. The C-terminus of GAT1-SSS brought down considerably less  $\beta$ -COP than the wild-type C-terminus (Fig. 5F).

### **GAT1-SSS punctae are part of the anterograde secretory pathway**

The hypothetical scenario outlined above also predicts that the GAT1-SSS-containing structures must be part of the anterograde secretory pathway. Thus, these containers ought to be accessible for an anterograde cargo en route to the Golgi. We employed the temperature-sensitive variant VSVG-ts045: this protein is misfolded at 40°C (Zilberstein et al., 1980) but rapidly refolds at the permissive temperature, concentrates into ERES and is exported. Thus, ER-to-Golgi transport can be readily synchronized. HEK293 cells were transfected with plasmids encoding YFP-tagged VSVG-ts045 and CFP-tagged GAT1-SSS. Cells were incubated at 40°C for 18-20 hours to accumulate VSVG-ts045 in the ER (Fig. 6A). As anticipated, under these restrictive conditions, YFP-VSVG-ts045 did not colocalize with GAT1-SSS (Fig. 6A). At 20 minutes after the cells had been shifted to the permissive temperature, YFP-VSVG-ts045 was enriched in ERGIC-like structures, which colocalized with GAT1-SSS punctae (Fig. 6B). At 30 minutes after the temperature shift, YFP-VSVG-ts045 was predominantly in a structure most compatible with the Golgi and it did not colocalize with GAT1-SSS (Fig. 6C). At these time points, YFP-VSVG-ts045 had already acquired, in part, resistance to endoglycosidase H (inset in the middle image of Fig. 6C). By contrast, GAT1-SSS was sensitive to endoglycosidase H (inset in the left image of Fig. 6C). These observations further support the interpretation that YFP-VSVG-ts045 had reached the Golgi and that GAT1-SSS was confined to a pre-Golgi compartment.

### **GAT1-SSS can be retrieved to the ER by addition of a dilysine motif**

Taken together, the results summarized in Fig. 6 demonstrate that components of the anterograde secretory pathway have access to the GAT1-SSS-containing structures. The ERGIC is a compartment in which sorting decisions are made (Appenzeller-Herzog and Hauri, 2006). Accordingly, components of the retrograde pathway must also have access to this compartment. We tested this prediction by extending the C-terminal end of GAT1-SSS with the four amino acids KKAA, giving rise to the mutant GAT1-SSS-KK, because the

sequence element KKXX is the prototypical retrograde-sorting motif. Upon expression, GAT1-SSS-KK was localized in the ER of HEK293 cells (Fig. 7A). To demonstrate that GAT1-SSS-KK was still capable of exiting the ER, we treated the cells with BFA for 2 hours. Under this condition, COPI-mediated retrieval of cargo from the ERGIC is blocked but COPII function is unaffected (Lippincott-Schwartz et al., 1989; Guo and Linstedt, 2006). Under BFA treatment, GAT1-SSS-KK was localized again in punctate structures (Fig. 7B). To show that BFA indeed acted on these cells, the same experiment was performed with cells co-expressing YFPGolgi, which was redistributed to the ER upon BFA treatment (Fig. 7D). Washout of BFA resulted in redistribution of GAT1-SSS-KK to the ER (Fig. 7C) while the Golgi fully recovered (Fig. 7E).

### Localization of GAT1-SSS in neurons

Finally, we ruled out that the observations with GAT1-SSS resulted from heterologous expression, i.e. its presence in cells that do not physiologically express neurotransmitter transporters (HEK293, HeLa and IdIF cells). Therefore, we expressed GAT1-SSS in hippocampal neurons of foetal rats [embryonic day (E)18] that had been allowed to differentiate for 7 days. At 48 hours after transfection, neurons were fixed and GAT1-SSS was imaged by confocal microscopy. GAT1-SSS showed a punctate distribution both in the soma and in neurite extensions of hippocampal neurons (Fig. 8).

### Discussion

In our previous work we showed that ER export of GAT1 is contingent on the <sup>566</sup>RL<sup>567</sup> motif in its C-terminus, which mediates interaction with Sec24D (Farhan et al., 2007). Here, we uncover a second adjacent motif, disruption of which causes retention of the mutant transporter (GAT1-SSS) in a pre-Golgi compartment that fulfils bona fide criteria of the ERGIC. This is supported by the following arguments: (i) GAT1-SSS was exported from the ER and was localized in a post-ER compartment. (ii) Transport of GAT1-SSS to this compartment was dependent on COPII. (iii) GAT1-SSS was not localized in the Golgi (lack of colocalization and presence of endoglycosidase H sensitivity). (iv) The compartment in which GAT1-SSS was localized was accessible to the machineries of both the anterograde and the retrograde secretory pathway; this is in agreement with the stable-compartment hypothesis, which posits that the ERGIC is a compartment in which antero- and retrograde cargoes are segregated from each other. (v) Treatment of cells with BFA caused GM130 to move to GAT1-SSS punctate structures.

We rule out that GAT1-SSS is severely misfolded and that its subcellular distribution reflects its localization in 'degradation containers' because: (i) its mobility in ER membranes is similar to that of wild-type GAT1, suggesting that it is not bound to chaperones, which would make it heavier and reduce its mobility. (ii) The formation of the punctate structures was dependent on COPII, because it was prevented by disruption of COPII assembly by introducing mutant Sec24D, which did not bind GAT1, and by mutation of the Sec24D-interaction motif in GAT1-SSS. The dependence of punctate structures on COPII function is not typical of a degradation compartment. (iii) We did not observe any toxic effect of GAT1-SSS on the secretory pathway: neither the morphology of the cell was

affected to any appreciable extent nor was the ability of the cell to support efficient trafficking of a different cargo, namely VSV-G, impaired. Finally, it appears highly unlikely that we introduced an artificial retention motif by introducing three serines in GAT1-SSS. In fact, if anything, the serine substitutions are predicted to facilitate anterograde trafficking to the plasma membrane: O'Kelly et al. (O'Kelly et al., 2002) showed that 14-3-3 $\beta$  binds to phosphoserine residues in the KCNK3 potassium channel and the major histocompatibility antigen class II-associated invariant chain Iip35. This binding overcomes  $\beta$ -COP-mediated retention. Thus, if we had created an artificial 14-3-3-binding motif, GAT1-SSS would be efficiently transported to the Golgi rather than retained in the intermediate compartment.

Under steady-state conditions, YFP-GAT1 did not colocalize with ERGIC53. Our parsimonious explanation assumes that GAT1-SSS leaves the ER via COPII vesicles, which fuse homotypically to give rise to larger containers. Further transport of GAT1-SSS is blocked and these containers thus become a dead-end for the transporter, because GAT1-SSS is an anterograde cargo that cannot move back to the ER. By contrast, ERGIC53 cycles continuously between the ERGIC and the ER. Under these assumptions, colocalization of ERGIC53 and GAT1-SSS is predicted to be poor. If, however, recycling of ERGIC53 is blocked (15°C block in HEK293 cells or 40°C in IdIF cells), ERGIC53 only moves in the anterograde direction and is therefore predicted to be also trapped in containers of the intermediate compartment in a manner similar to GAT1-SSS: accordingly, under these conditions, the two proteins colocalize in the same membrane containers. An alternative explanation is to assume that GAT1-SSS resides in pre-Golgi intermediates that are negative for ERGIC53. There is recent evidence for the existence of ERGIC elements that do not contain ERGIC53 (Sannerud et al., 2006): upon differentiation, PC12 cells develop neurite extensions and expand the ERGIC; RAB1-containing tubules thereof extend to the growth cones of the neurite extensions, whereas ERGIC53-positive ERGIC elements remain in the cell body. Similarly, it was reported earlier that p58 (the rat homologue of ERGIC53) is only found in the soma of rat hippocampal neurons but not in dendrites or axons (Krijnse-Locker et al., 1995). As a neurotransmitter transporter, GAT1 is targeted to the axon in neurons and we have previously shown that it is enriched in the growth cone and the neurite extension of PC12 cells (Farhan et al., 2004). Here, we show that GAT1-SSS is localized in punctated structures in hippocampal neurons. These structures can be found in both the soma and in neuronal extensions. Therefore, it is tempting to speculate that GAT1 moves, in principle, through ERGIC53-negative ERGIC-like elements. This hypothetical model predicts that ERGIC53 and the ERGIC-retained mutant of GAT1 do not colocalize and their colocalization is forced by manipulations that perturb the functional segregation of individual ERGIC domains.

Finally, in this study, we observed that trafficking of GAT1 from the ERGIC was controlled by its C-terminus. It remains to be tested whether other proteins require specific sorting elements to exit the ERGIC. If this were the case, it would lend additional support for the stationary-compartment hypothesis, i.e. the notion that the ERGIC is a stable compartment in which sorting decisions are made rather than a collection of homotypically fusing vesicles that segregate into containers moving either in the anterograde or retrograde direction.



## Materials and Methods

### Materials, reagents and mutagenesis

The plasmid encoding YFP-Sec24D was a gift from R. Pepperkok (European Molecular Biology Laboratory, Heidelberg, Germany). The plasmid encoding hamster Sar1a was a gift from W. E. Balch (The Scripps Research Institute, La Jolla, USA). Sar1a-T39N was generated using the QuickChange II XL site-directed mutagenesis kit (Stratagene). The plasmid encoding CFP-tagged reticulon 2 was a gift from J. D. Rothstein (Johns Hopkins University, MD). Polyclonal anti-G and monoclonal anti-GM130 antibodies were from BD-Clontech. Polyclonal anti-Sec31 antibody was a gift from F. Gorelick (Yale University School of Medicine, CT). Brefeldin A (BFA) was purchased from Sigma. YFP-Golgi, which is a YFP-tagged targeting sequence of human  $\beta$ 1,4-galactosyltransferase, was purchased from BD-Clontech; IdIF cells were a gift from M. Krieger (MIT, Cambridge, MA).

### Cell culture and transfection

HEK293 cells were cultured in Dulbecco's modified Eagle's medium (DMEM) supplemented with 10% foetal bovine serum, L-glutamine and antibiotics. For microscopy,  $0.3 \times 10^6$  cells were seeded on poly-D-lysine-coated coverslips. Transient transfections were done with the CaPO<sub>4</sub> precipitation method. Only in the case of budding assays, cells were transiently transfected using Lipofectamine-Plus (Invitrogen). IdIF cells were cultured in Ham's F-12 medium supplemented with glutamine, 5% foetal bovine serum and antibiotics. Cells were maintained at 34°C.

### Preparation of rat hippocampal neurons

High-density cultures ( $\sim 50,000$  cells/cm<sup>2</sup>) were established from E18 Wistar-rat hippocampi. The foetal hippocampi were removed from the brain, washed once in HBSS and trypsinized for 15 minutes at 37°C. Afterwards, hippocampi were washed again in HBSS followed by additional washes in pre-warmed plating medium (DMEM/Glutamax, 0.6% glucose, 10% foetal calf serum and antibiotics). Finally, the hippocampi were dissociated in the plating medium on glass coverslips (pre-coated with poly-L-lysine; 1 mg/ml in borate buffer, pH 8.5; coated overnight and washed twice with water). After 3 hours from the initial seeding, the medium was changed to Neurobasal medium (Gibco) supplemented with 0.5 mM glutamine, antibiotics and B27 supplement (Gibco). Neurons were transfected after 7 days in vitro using lipofectamine 2000 (Invitrogen) according to the manufacturer's instructions.

### GST pull-down

Purified fusion proteins (10  $\mu$ g) comprising GST and the wild-type C-terminal of GAT1 or its SSS-mutated version were incubated at 4°C for 30 minutes with 100  $\mu$ g of cytosol from HEK293 cells. Glutathione agarose beads were subsequently added (50  $\mu$ l slurry) and the sample was filled up to 500  $\mu$ l with buffer (25 mM HEPES-KOH, pH 7.2, 130 mM KCl). Samples were further incubated for 2 hours at 4°C. Beads were centrifuged and washed twice with buffer (25 mM HEPES-KOH, pH 7.2, 130 mM KCl). Proteins were eluted from

beads by boiling in sample buffer. A 50% aliquot of the eluate was loaded onto a SDS-polyacrylamide gel.

### Fluorescence microscopy

Fluorescence images were captured at room temperature with a Zeiss Axiovert 200M inverted epifluorescence microscope equipped with a CoolSNAP fx cooled CCD camera (Photometrics, Roper Scientific). The fluorescence filters used on this setup were purchased from Chroma Technology Corporation. For confocal microscopy, cells were examined with a 40× oil immersion objective with a Zeiss LSM510 confocal microscope. For immunofluorescence microscopy, cells were fixed in 4% paraformaldehyde for 30 minutes at room temperature. ERGIC53 was visualized by indirect immunofluorescence using the murine monoclonal antibody G1/93, which is directed against ERGIC53 (Schweizer et al., 1988), at a dilution of 1:1000 and an Alexa-Fluor-568-labelled anti-mouse antibody (Molecular Probes) at a dilution of 1:1000.

### In vitro budding assay

HEK293 cells in 10-cm culture dishes were transfected with the plasmids specified in the pertinent figure legends using Lipofectamine-Plus (Invitrogen). After 24 hours, cells were permeabilized by a 5-minute incubation in hypotonic buffer containing 18 mM KOAc and 18 mM Tris-HCl, pH 7.2 (Schwaninger et al., 1992); these cells are referred to as semi-intact cells. The budding reaction was done according to Xu and Hay (Xu and Hay, 2004) with the following adaptations (see also Farhan et al., 2007): the reaction mixture consisted of 25  $\mu$ l semi-intact cells ( $8 \times 10^5$  cells/reaction), 60  $\mu$ l cytosol (3-4  $\mu$ g/ $\mu$ l), 20  $\mu$ l buffer (18 mM CaOAc, 50 mM EGTA, 20 mM HEPES-KOH, pH 7.2), 5  $\mu$ l 0.1 M MgOAc, 22  $\mu$ l H<sub>2</sub>O, 58  $\mu$ l 25/125 buffer (125 mM KOAc, 25 mM HEPES-KOH, pH 7.2) and 10  $\mu$ l GMP-PNP (final concentration was 20  $\mu$ M). Reactions were incubated at 37°C with mild shaking for 100 minutes. Cells were harvested by centrifugation at 1500 g for 5 minutes, resuspended in 30  $\mu$ l 25/70 buffer (70 mM KOAc, 25 mM HEPES-KOH, pH 7.2) and centrifuged at 12,000 g for 5 minutes. The supernatant represented the vesicular fraction, whereas the pellet contained heavier membranes (e.g. ER, Golgi etc.). If the formation of punctate structures by GAT1-SSS was to be visualized microscopically, the same conditions were maintained with the exception that 25  $\mu$ l of 25/90 buffer was used instead of cells and the reaction was performed in the presence of an ATP-regeneration system (5 mM creatine phosphate, 4 ng/ml creatine kinase, 1 mM ATP, 0.5 mM GTP). The cytosol employed in these complementation experiments was prepared from control cells and from appropriately transfected cells ( $4 \times 10^7$ ) by sonication in 0.4 ml buffer (20 mM Tris-HCl, pH 7.2, 130 mM KCl). The particulate material was removed by centrifugation (70 minutes at 40,000 g).

### Fluorescence recovery after photobleaching (FRAP)

FRAP was recorded on a Zeiss LSM510 confocal laser scanning microscope. Transfected cells were examined with an oil immersion objective (40× magnification). Circular regions of interest were selected for bleaching and scanning (bleach regions). Before bleaching, a scan was obtained; the area of interest was then bleached with 70 iterations at maximum laser power (30 mW at 514 nm). Subsequently, pictures were captured (50 scans in 40

seconds) with 4% of laser power. The recorded fluorescence intensities were digitized and averaged over the bleach region using ImageJ 1.37c; these values were plotted and subjected to non-linear curve fitting to the equation describing the monoexponential rise to a maximum:  $y = \text{bottom} + (\text{top} - \text{bottom}) \times (1 - e^{-kx})$ , where bottom refers to the relative fluorescence intensity immediately after bleaching (before recovery) and top to the value that is reached at equilibrium (after recovery).

## Electron microscopy

Cells grown on coverslips as described above were fixed in 2.5% glutaraldehyde buffered to pH 7.4 in 0.1 M sodium cacodylate for 1 hour at 4°C. After an overnight rinse in the same buffer, cells were post-fixed in 1% veronal-acetate-buffered OsO<sub>4</sub> for 2 hours, dehydrated in a graded series of ethanol and embedded in Epon. Ultrathin sections were examined in a transmission electron microscope, either unstained or stained in alcoholic uranyl acetate and alkaline lead citrate.

## Acknowledgments

This work was supported by a grant from the Austrian National Bank to H.F. (10507) and by the Austrian Science Foundation (FWF) grants P18072 (to H.F.) and P18706 (to H.H.S.). The excellent technical assistance of Elfriede Scherzer and Ulrich Kaindl is gratefully acknowledged.

## References

- Alvarez C, Garcia-Mata R, Brandon E, Sztul E. COPI recruitment is modulated by a Rab1b-dependent mechanism. *Mol. Biol. Cell.* 2003; 14:2116–2127. [PubMed: 12802079]
- Appenzeller-Herzog C, Hauri HP. The ER-Golgi intermediate compartment (ERGIC): in search of its identity and function. *J. Cell Sci.* 2006; 119:2173–2183. [PubMed: 16723730]
- Aridor M, Balch WE. Kinase signaling initiates coat complex II (COPII) recruitment and export from the mammalian endoplasmic reticulum. *J. Biol. Chem.* 2000; 275:35673–35676. [PubMed: 11001944]
- Ben-Tekaya H, Miura K, Pepperkok R, Hauri HP. Live imaging of bidirectional traffic from the ERGIC. *J. Cell Sci.* 2005; 118:357–367. [PubMed: 15632110]
- Farhan H, Korkhov VM, Paulitschke V, Dorostkar MM, Scholze P, Kudlacek O, Freissmuth M, Sitte HH. Two discontinuous segments in the carboxyl terminus are required for membrane targeting of the rat gamma-aminobutyric acid transporter-1 (GAT1). *J. Biol. Chem.* 2004; 279:28553–28563. [PubMed: 15073174]
- Farhan H, Reiterer V, Korkhov VM, Schmid JA, Freissmuth M, Sitte HH. Concentrative export from the ER of the GABA-transporter 1 requires binding to SEC24D. *J. Biol. Chem.* 2007; 282:7679–7689. [PubMed: 17210573]
- Gomez M, Scales SJ, Kreis TE, Perez F. Membrane recruitment of coatamer and binding to dilysine signals are separate events. *J. Biol. Chem.* 2000; 275:29162–29169. [PubMed: 10864930]
- Guo Y, Linstedt AD. COPII-Golgi protein interactions regulate COPII coat assembly and Golgi size. *J. Cell Biol.* 2006; 174:53–63. [PubMed: 16818719]
- Hauri HP, Kappeler F, Andersson H, Appenzeller C. ERGIC-53 and traffic in the secretory pathway. *J. Cell Sci.* 2000; 113:587–596. [PubMed: 10652252]
- Horstmann H, Ng CP, Tang BL, Hong W. Ultrastructural characterization of endoplasmic reticulum-Golgi transport containers (EGTC). *J. Cell Sci.* 2002; 115:4263–4273. [PubMed: 12376558]
- Krijnse-Locker J, Parton RG, Fuller SD, Griffiths G, Dotti CG. The organization of the endoplasmic reticulum and the intermediate compartment in cultured rat hippocampal neurons. *Mol. Biol. Cell.* 1995; 6:1315–1332. [PubMed: 8573789]

- Lippincott-Schwartz J, Yuan LC, Bonifacino JS, Klausner RD. Rapid redistribution of Golgi proteins into the ER in cells treated with brefeldin A: evidence for membrane cycling from Golgi to ER. *Cell*. 1989; 56:801–813. [PubMed: 2647301]
- Monetta P, Slavin I, Romero N, Alvarez C. Rab1b interacts with GBF1 and modulates both ARF1 dynamics and COPI association. *Mol. Biol. Cell*. 2007; 18:2400–2410. [PubMed: 17429068]
- Nakamura N, Rabouille C, Watson R, Nilsson T, Hui N, Slusarewicz P, Kreis TE, Warren G. Characterization of a cis-Golgi matrix protein, GM130. *J. Cell Biol*. 1995; 131:1715–1726. [PubMed: 8557739]
- O’Kelly I, Butler MH, Zilberberg N, Goldstein SA. Forward transport. 14-3-3 binding overcomes retention in endoplasmic reticulum by dibasic signals. *Cell*. 2002; 111:577–588. [PubMed: 12437930]
- Pepperkok R, Scheel J, Horstmann H, Hauri HP, Griffiths G, Kreis TE. Beta-COP is essential for biosynthetic membrane transport from the endoplasmic reticulum to the Golgi complex in vivo. *Cell*. 1993; 74:71–82. [PubMed: 8334707]
- Sannerud R, Marie M, Nizak C, Dale HA, Pernet-Gallay K, Perez F, Goud B, Saraste J. Rab1 defines a novel pathway connecting the pre-Golgi intermediate compartment with the cell periphery. *Mol. Biol. Cell*. 2006; 17:1514–1526. [PubMed: 16421253]
- Schwanninger R, Plutner H, Davidson HW, Pind S, Balch WE. Transport of protein between endoplasmic reticulum and Golgi compartments in semiintact cells. *Meth. Enzymol*. 1992; 219:110–124. [PubMed: 1336806]
- Schweizer A, Fransen JA, Bachi T, Ginsel L, Hauri HP. Identification, by a monoclonal antibody, of a 53-kD protein associated with a tubulo-vesicular compartment at the cis-side of the Golgi apparatus. *J. Cell Biol*. 1988; 107:1643–1653. [PubMed: 3182932]
- Schweizer A, Ericsson M, Bachi T, Griffiths G, Hauri HP. Characterization of a novel 63 kDa membrane protein. Implications for the organization of the ER-to-Golgi pathway. *J. Cell Sci*. 1993; 104:671–683. [PubMed: 8314869]
- Tobler AR, Notterpek L, Naef R, Taylor V, Suter U, Shooter EM. Transport of Trembler-J mutant peripheral myelin protein 22 is blocked in the intermediate compartment and affects the transport of the wild-type protein by direct interaction. *J. Neurosci*. 1999; 19:2027–2036. [PubMed: 10066256]
- Xu D, Hay JC. Reconstitution of COPII vesicle fusion to generate a pre-Golgi intermediate compartment. *J. Cell Biol*. 2004; 67:997–1003. [PubMed: 15611329]
- Yu S, Satoh A, Pypaert M, Mullen K, Hay JC, Ferro-Novick S. mBet3p is required for homotypic COPII vesicle tethering in mammalian cells. *J. Cell Biol*. 2006; 174:359–368. [PubMed: 16880271]
- Zilberstein A, Snider MD, Porter M, Lodish HF. Mutants of vesicular stomatitis virus blocked at different stages in maturation of the viral glycoprotein. *Cell*. 1980; 21:417–427. [PubMed: 6250721]

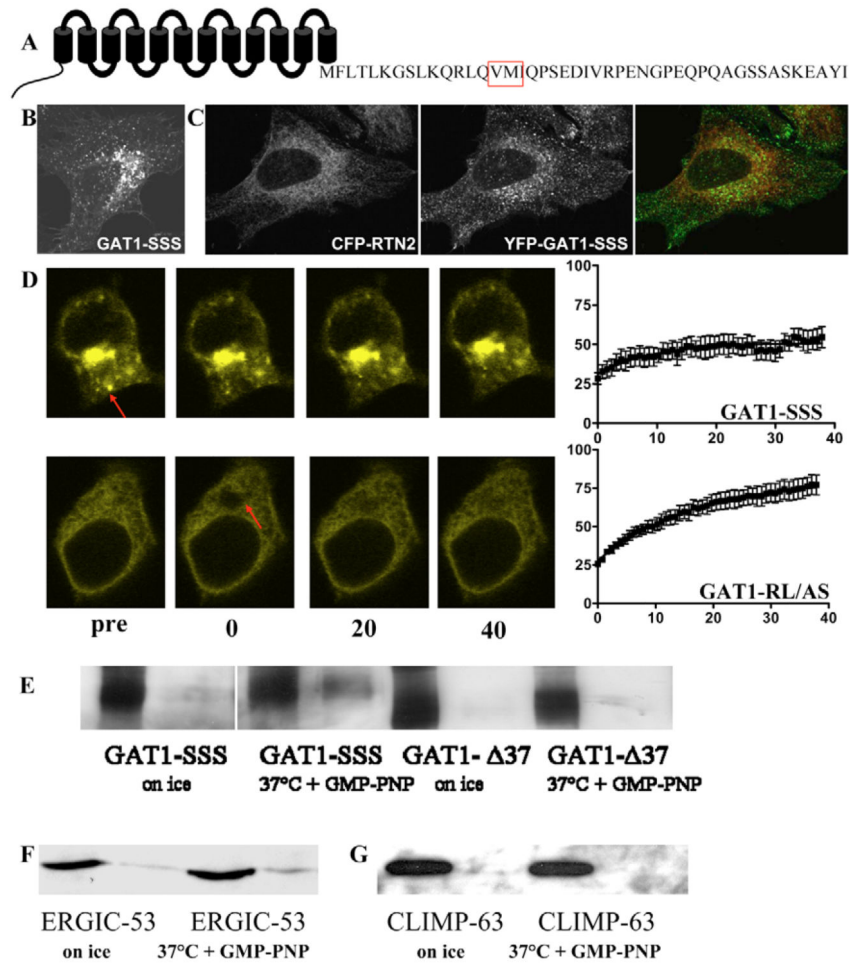


**Fig. 1.** Localization and transport of GAT1-SSS. (A) Schematic representation of GAT1 showing its 12 transmembrane segments and the C-terminus. The motif replaced by serines in the mutant GAT1-SSS is highlighted by the red box. (B) A HeLa cell expressing YFP-tagged GAT1-SSS. The image was captured 24 hours after transfection by confocal laser scanning microscopy (Leica SPE). (C) HeLa cells were co-transfected with plasmids encoding YFP-tagged GAT1-SSS and CFP-tagged reticulon 2 (CFP-RTN2). After 24 hours cells were fixed and imaged by confocal laser scanning microscopy (Leica SPE). Merged image is on the right. (D) HEK293 cells were transfected with plasmids encoding YFP-tagged GAT1-SSS (upper panels) or YFP-tagged GAT1-RL/AS (lower panels). Arrows indicate the bleached region. FRAP was recorded as described in the Materials and Methods. Fluorescence intensities were expressed as percentage of fluorescence measured prior to bleaching, and the data points were subjected to curvilinear regression using an equation for a monoexponential rise from a basal value to obtain the rate constant for fluorescence recovery and the mobile fraction. Data are means  $\pm$  s.e.m. from four or five independent experiments. (E) YFP-GAT1-SSS, or GAT1- $\Delta$ 37, and Sar1a-T39N were transiently co-expressed in HEK293 cells. On the next day, semi-intact cells were prepared and the in vitro budding assay was performed as described in the Materials and Methods. (F,G) Vesicle-

budding assay performed in semi-intact cells transfected with Sar1a-T39N. Budding of endogenous ERGIC-53 (F) and CLIMP-63 (G) was determined as in panel E.

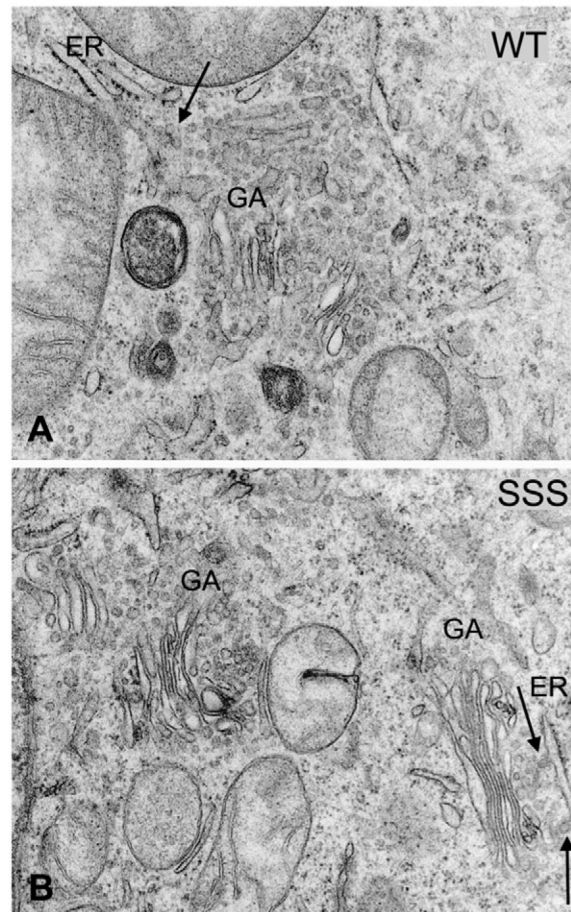


**Fig. 2.** Ultrastructure of HEK293 cells expressing wild-type (WT) GAT1 (A) and GAT1-SSS (B). Cells grown on glass coverslips were fixed in 2.5% glutaraldehyde, pH 7.4, post-fixed in 1% veronal-acetate-buffered OsO<sub>4</sub>, dehydrated in a graded series of ethanol and embedded in Epon. The electron micrographs show parts of the paranuclear cytoplasm, in which cisternae of the ER, ER exit sites (arrows) and Golgi apparatus stacks (GA) are visible. Magnification was 33,000 $\times$  (A,B).

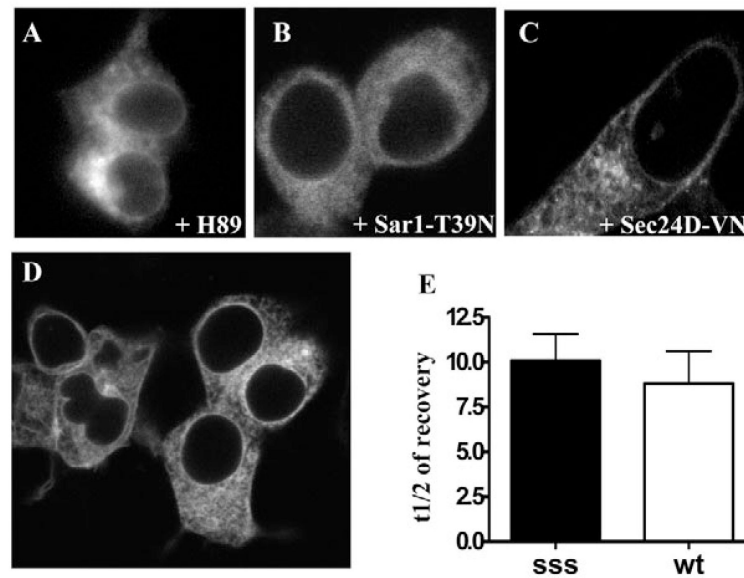


**Fig. 3.**

Accumulation of GAT1-SSS in punctate structures requires the COPII-dependent ER-export machinery. (A) HEK293 cells were transfected with a plasmid encoding YFP-tagged GAT1-SSS. Cells were treated overnight with H89 (100 μM). Images were acquired 24 hours after transfection. (B,C) HEK293 cells were co-transfected with plasmids coding for CFP-tagged GAT1-SSS (1 μg) and Sar1-T39N (2 μg, B) or YFP-tagged Sec24D-VN (2 μg, C). Images were acquired 24 hours after transfection. (D) HEK293 cells were transfected with a plasmid coding for the double mutant YFP-tagged GAT1-RL/AS-SSS and images were captured 24 hours after transfection. (E) HEK293 cells were co-transfected with plasmids encoding SAR1A-T39N (2 μg) and either YFP-tagged wild-type GAT1 (wt; 1 μg) or YFP-tagged GAT1-SSS (sss; 1 μg). FRAP was recorded as outlined in the Materials and Methods. Data represent mean half-lives in seconds of fluorescence recovery from five independent experiments; error bars indicate s.e.m.



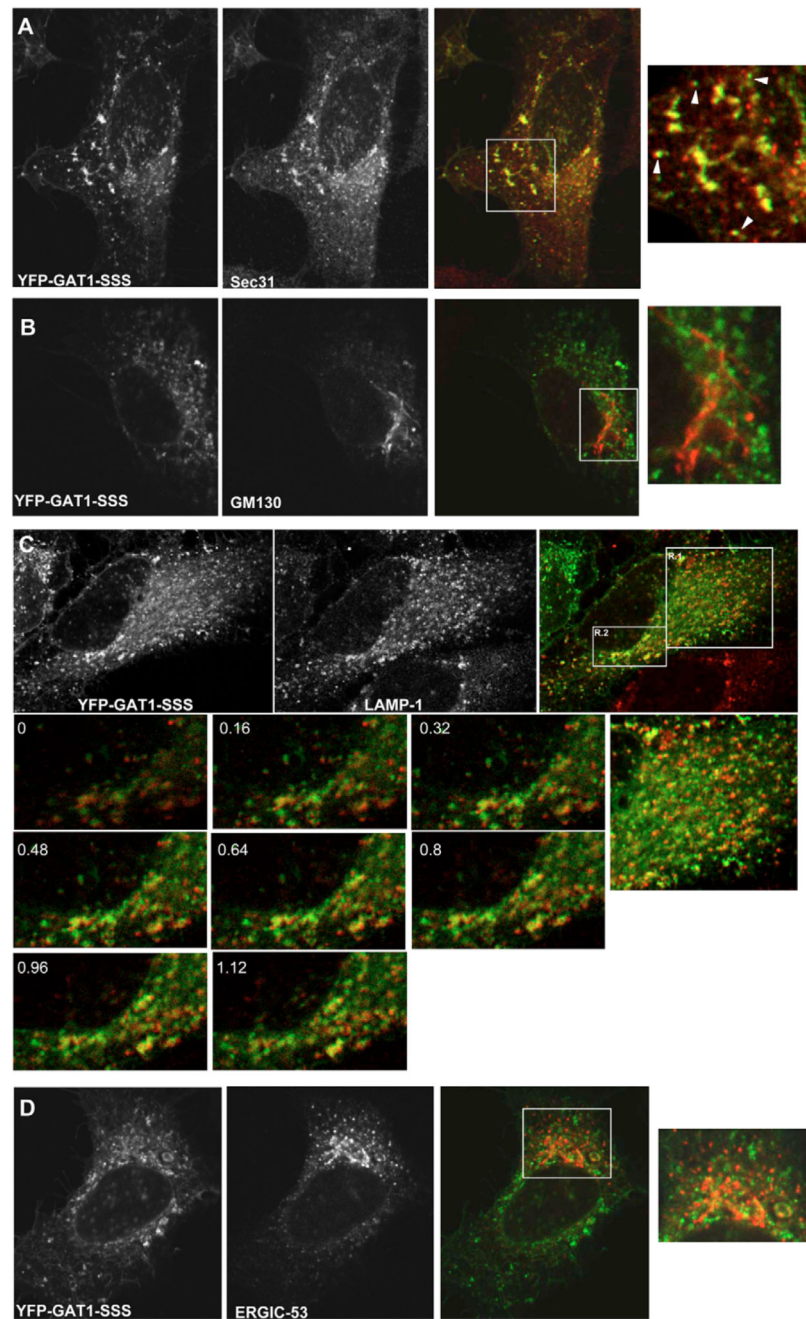


**Fig. 4.** Colocalization of GAT1-SSS with subcellular markers. HeLa cells were transfected with plasmids encoding YFP-tagged GAT1-SSS. After 24 hours, cells were fixed and immunostained against the ERES marker Sec31 (A), the cis-Golgi marker GM130 (B), the late endosome/lysosome marker LAMP1 (C) and a marker for the intermediate compartment, ERGIC53 (D). (A,B,D) Boxed areas are shown as close-ups on the right. (A) Arrowheads highlight GAT1-SSS puncta that are closely associated with ERES. (C) The numbered images represent magnifications of region 2 (R.2), which were acquired in

multiple optical slices. The numbers indicate how many  $\mu\text{m}$  the optical slices are from 0. To the right of these is a close-up of region 1 (R.1). Images were acquired using a confocal microscope (Leica SPE).

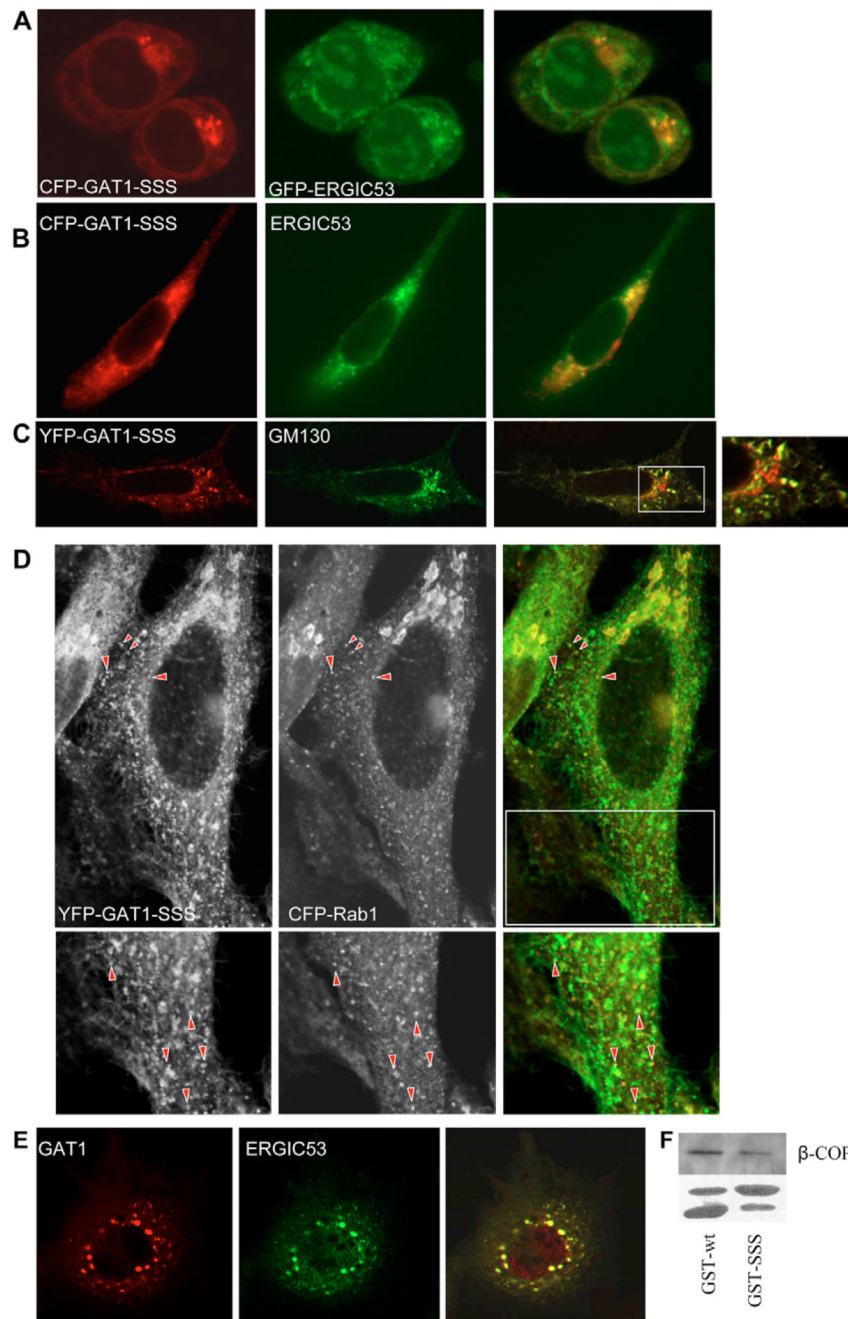


**Fig. 5.** GAT1-SSS localizes to the ERGIC. (A) HEK293 cells co-expressing CFP-GAT1-SSS and GFP-ERGIC53 were incubated at 15°C for 2 hours. Cells were fixed and images were subsequently captured by confocal microscopy (Zeiss LSM 510). Overlays (right) were generated using the Zeiss LSM image browser. (B) LdlF cells were co-transfected with plasmids encoding CFP-tagged GAT1-SSS and GFP-tagged ERGIC53. Cells were maintained at 34°C for 20 hours. Thereafter, the temperature was shifted to 40°C for 5 hours; subsequently, the images were captured with a CCD camera, digitized and overlaid

(right) using MetaMorph software. (C) HeLa cells were transfected with a plasmid encoding YFP-tagged GAT1-SSS. After 24 hours, cells were treated with BFA (5  $\mu\text{g/ml}$ ) for 10 minutes at 37°C. Afterwards, cells were fixed and GM130 was detected by immunofluorescence. Images were acquired using a confocal microscope (Leica SPE). The boxed area in the overlaid image is shown close-up on the right. (D) HeLa cells were co-transfected with plasmids encoding YFP-tagged GAT1-SSS and CFP-tagged RAB1. After 24 hours, cells were fixed. Images were acquired using a confocal microscope (Leica SP5). Raw images are displayed in grey to enhance visibility of the peripheral structures. Arrowheads highlight peripheral punctae showing colocalization. The lower panels show magnified views of the boxed region. (E) LdlF cells were co-transfected with plasmids encoding YFP-tagged wild-type GAT1 and myc-tagged ERGIC53. Cells were cultured at 34°C for 20 hours. Thereafter, the temperature was shifted to 40°C for 5 hours. Subsequently, cells were fixed and processed for immunofluorescence against the myc-epitope. (F) Cytosol from HEK293 cells (100  $\mu\text{g}$ ) was incubated with a fusion protein comprising GST and the GAT1 C-terminus (10  $\mu\text{g}$ ), either in its wild-type version (GST-wt) or that of mutated GAT1-SSS (GST-SSS). The GST-pull-down was performed as indicated in the Materials and Methods. The upper panel shows immunostaining for  $\beta$ -COP. In the lower panel, GST fusion proteins were visualized by staining with Ponceau red. The upper band represents the fusion protein of GST and C-terminus, whereas the lower band reflects proteolytic degradation and corresponds to the size of GST.

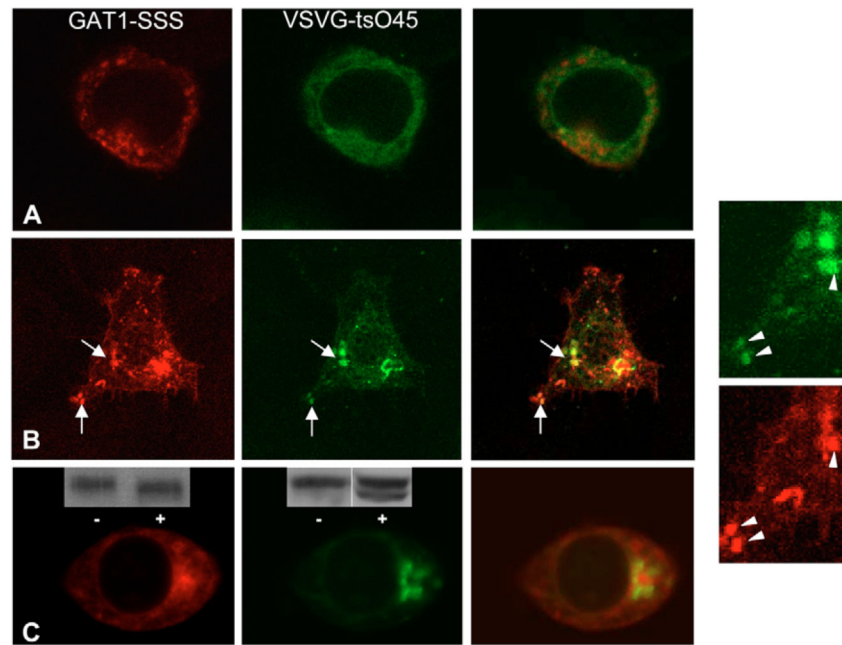


**Fig. 6.** Transient colocalization of YFP-tagged VSVG-ts045 with CFP-tagged GAT1-SSS during its trafficking through the anterograde secretory pathway. HEK293 cells were co-transfected with plasmids encoding CFP-tagged GAT1-SSS and YFP-tagged VSVG-ts045. Cells were incubated for 20 hours at 40°C. Images were acquired using a confocal microscope before (A) and at 10 (B) and 30 (C) minutes after shifting to the permissive temperature. The two images on the right show close-ups of those in B. (C) Insets show immunoblots of CFP-tagged GAT1-SSS (left-hand panel) and YFP-tagged VSVG-ts045 (middle panel): cell extracts were prepared at 30 minutes after shifting to the permissive temperature and incubated overnight in the absence (-) or presence (+) of endoglycosidase H. Immunoreactive material was visualized by an antiserum directed against GFP.

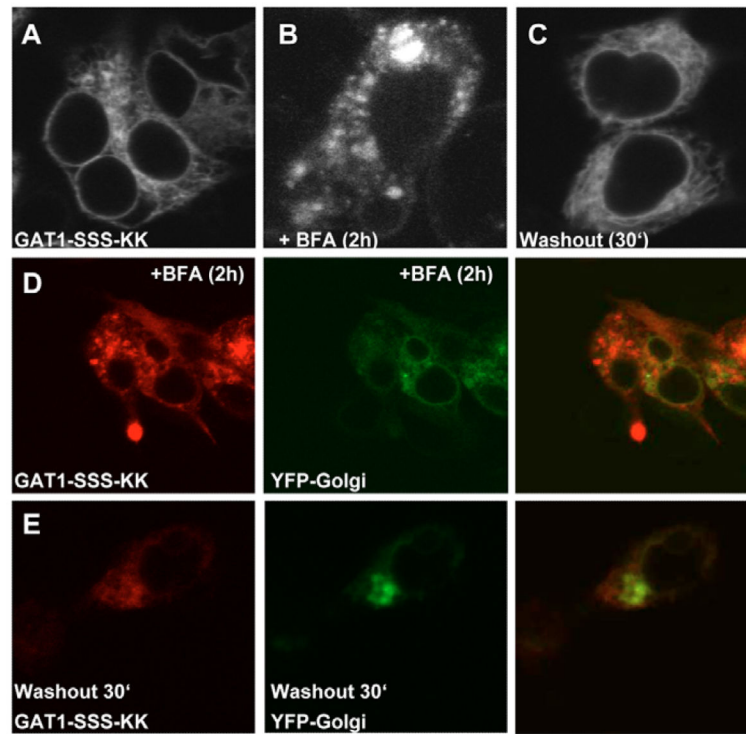


**Fig. 7.** Attaching a dilysine motif to GAT1-SSS supports its retrieval to the ER. (A) HEK293 cells were transfected with plasmids encoding CFP-tagged GAT1-SSS-KK. Images were acquired 24 hours later with a confocal microscope. (B,C) HEK293 cells expressing CFP-tagged GAT1-SSS-KK treated with 10 μg/ml BFA for 2 hours (B) and at 30 minutes after washout of BFA (C). (D,E) HEK293 cells co-expressing GAT1-SSS-KK and YFP-Golgi treated with 10 μg/ml BFA for 2 hours (D) and at 30 minutes after washout (E).

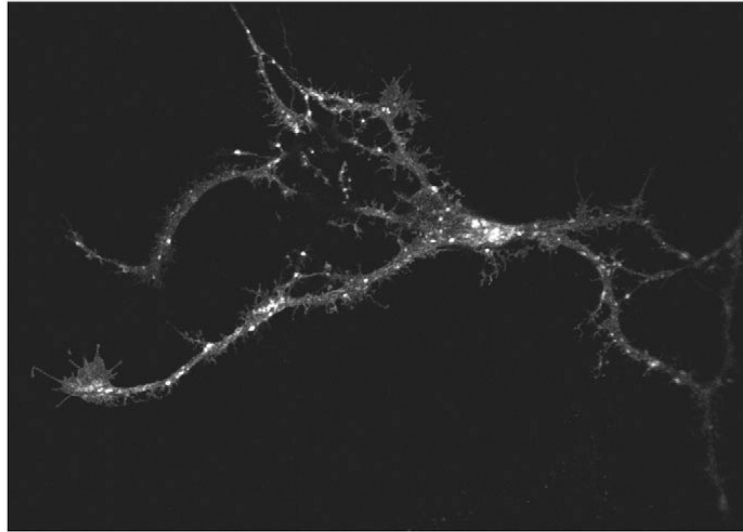


**Fig. 8.** Localization of GAT1-SSS in hippocampal neurons. Hippocampal neurons were isolated from foetal rat brains (E18) and transfected after 7 days in culture using Lipofectamine 2000 with a plasmid encoding YFP-tagged GAT1-SSS. The transporter was visualized by confocal fluorescence microscopy 48 hours after transfection.